The Weakest Link: A Nodal Tension Model for Local Network Resilience

Anonymous authors
Paper under double-blind review

Abstract

The resilience of networked systems, defined by their ability to withstand targeted disruptions between a source and a target, is a critical concern in fields from ecology to infrastructure management. While spectral methods offer global insights, characterising the specific vulnerability of targeted pathways requires a more direct approach. In this paper, we frame this problem of local resilience through the powerful lens of linear duality, adopting the classic dual of the maximum $s-t$ flow problem and interpreting it through a novel physical analogy of "Nodal Tension". Our main theoretical results establish that (1) the model's optimal value is exactly equal to the capacity of the minimum $s-t$ cut, and (2) an optimal vertex solution exists where all node potentials are integer-valued ($\{0,1\}$), thus revealing the precise combinatorial structure of the cut. We validate these theorems computationally against standard algorithms. We then apply our model to a real-world conservation problem: assessing the connectivity of a grizzly bear corridor in the Canadian Rocky Mountains. The analysis reveals a novel ecological insight: the corridor's weakest link is not a remote bottleneck, but the local perimeter of the source protected area itself. This "null signal" for a classic choke point challenges conventional conservation paradigms and demonstrates our model's utility in generating non-obvious, actionable scientific discoveries. Our work provides a complete polyhedral characterisation of local network resilience, offering a computationally efficient and scientifically interpretable tool. Code to reproduce all results is available at https://anonymous.4open.science/r/tmlr-ldnr

1 Introduction

In an era of unprecedented habitat fragmentation, analysing the connectivity of ecological landscapes has become a central challenge in conservation science (Vorosmarty et al., 2000). Current analytical approaches generally fall into two distinct paradigms. The first, and most common in applied conservation, focuses on path-finding, using methods like least-cost path analysis to identify optimal wildlife corridors between specific locations (Rosenberg et al., 1997; Hilty et al., 2020). The second, rooted in spectral graph theory, assesses the global health of the entire network, using metrics like algebraic connectivity to quantify its overall robustness to disruption (Chung, 1997). While both paradigms provide valuable ecological information, neither directly answers a crucial third question: *what is the resilience of the specific connection between two chosen protected areas, and where is its absolute weakest link*? In this paper, we argue that this question of localised, pairwise resilience represents a distinct and vital mode of network analysis. To this end, we introduce a framework to formalise this concept and demonstrate that focusing on this local resilience can lead to fundamentally different and novel insights for conservation management.

Current methods for analysing network structure, while powerful, often present a mismatch for such targeted questions. Spectral graph theory, for instance, provides global measures of connectivity through the algebraic connectivity (λ_2, the Fiedler vector), which is fundamentally linked to the graph's sparsest cut via Cheeger's inequality (Chung, 1997). While invaluable for assessing overall network robustness, these global measures do not directly identify the specific weakest link between a given source and target. Semidefinite programming (SDP) relaxations offer the tightest known approximations for the general sparsest cut problem (Arora et al., 2009), but their computational expense and conceptual complexity can be prohibitive for environmental

practitioners. The critical gap is the need for a simple, scalable, and interpretable model that directly solves the local resilience problem: *finding the minimum cut that severs the connection between a specific source node s and a target node t.*

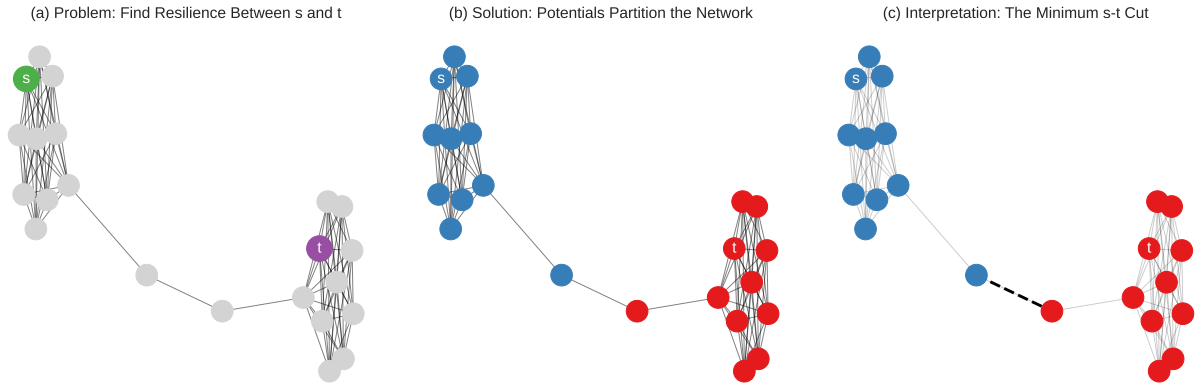

Figure 1: Illustration of our Nodal Tension model for local network resilience. **(a)** The problem is to quantify the resilience of the connection between a source node (s) and a target node (t) in a network with a clear weakest link. **(b)** Our linear program solves for a potential at each node. The optimal potentials, proven to be integer-valued ($\{0, 1\}$), partition the network's nodes into two distinct sets (blue and red). **(c)** The interpretation of this partitioning is the minimum $s - t$ cut. The single edge crossing the partition (dashed line) represents the most critical link, and its capacity, the optimal value Z^*, provides a direct, quantitative measure of the pathway's resilience.

Our core idea is to frame this local resilience problem using the elegant lens of linear duality. We adopt the classic linear programming dual of the maximum-flow problem, interpreting it through a novel physical analogy which we term the "Nodal Tension" model, providing a potential-based perspective on a classic optimisation problem (illustrated in Figure 1). Instead of modelling flows, our primal LP assigns a scalar potential p_i to each node in the network. The objective is to minimise the total tension across all edges—defined as the sum of potential differences—subject to a fixed potential difference between a designated source s and target t. This intuitive physical analogy of stretching a network provides a powerful yet simple framework. We show that this potential-based primal formulation is the linear dual of the classic maximum $s - t$ flow problem, thereby building a new bridge between a physical interpretation and a cornerstone of combinatorial optimisation.

This primal-dual perspective allows us to establish a complete theoretical characterisation of local network resilience. Our main theoretical contributions are twofold. First, leveraging the max-flow min-cut theorem (Ford Jr & Fulkerson, 1956; Kleinberg & Tardos, 2006) and strong LP duality, we prove that the optimal value of our min-tension LP is exactly equal to the capacity of the minimum $s - t$ cut. Second, we prove a powerful integrality theorem. By demonstrating that the LP's constraint matrix is totally unimodular, we prove that an optimal solution exists where all node potentials are integer-valued ($\{0, 1\}$). This is a crucial result, as it shows that the continuous optimisation perfectly recovers the discrete, combinatorial structure of the cut, directly partitioning the network's nodes into two distinct sets.

We conduct a comprehensive experimental validation to support our theory. We first validate our model's correctness by showing that its output is identical to that of a standard Edmonds-Karp max-flow algorithm on benchmark flow networks. We then computationally verify our integrality theorem across a diverse range of graph topologies, demonstrating that the optimal potentials are consistently binary. Finally, we showcase the model's practical utility in a compelling real-world case study. Using geospatial habitat data, we construct a connectivity network for grizzly bears in the Northern Rocky Mountains and apply our model to identify the most critical and vulnerable choke points in the habitat corridor between the Yellowstone and Selkirk ecosystems, providing actionable insights for conservation planning.

Our primary contributions in this paper are:

- A rigorous formulation of local network resilience, the Nodal Tension model, which interprets the classic dual of the max-flow problem through an intuitive physical analogy.
- A complete theoretical characterisation of this model, proving its exact equivalence to the minimum $s-t$ cut and the guaranteed integrality of its solution, which ensures the recovery of the combinatorial cut structure.
- A comprehensive experimental validation of the model's correctness and theoretical properties against standard benchmarks.
- A quantitative ecological finding from a real-world case study, demonstrating the absence of a remote corridor choke point and revealing that local connectivity at a protected area's boundary can be the true weakest link.

This paper is structured as follows. We review prior work in Section 2. In Section 3, we formally define our Nodal Tension LP. We present our main theoretical results in Section 4. The validation experiments and grizzly bear case study are detailed in Section 5. We conclude with a discussion in Section 6. Detailed proofs are provided in the Appendix A.

2 Related Work

Our work is positioned at the intersection of several distinct but related fields. To properly situate our contribution, we first survey the broad, global perspectives on network resilience to establish the dominant paradigms. We then narrow our focus to the specific domain of ecological connectivity, highlighting the practical tools currently in use and their inherent focus on path-finding. Next, we examine the related but distinct field of graph partitioning, clarifying the difference between the unsupervised, global goal of community detection and our supervised, local goal. Finally, we review the foundational principles of Spectral Graph Theory and optimisation-based methods to demonstrate how our work offers a simpler, more direct, and more interpretable solution for the specific problem of local, pairwise resilience.

2.1 Network Resilience and Robustness

The study of network resilience, broadly concerned with the ability of a system to maintain its function in the face of perturbations, has deep roots in ecology (Holling et al., 1973) and has become a cornerstone of modern network science (Newman, 2018). Much of the foundational work has focused on understanding the topological underpinnings of robustness. The differing properties of random graphs (Bollobás, 2011) versus scale-free networks (Barabási & Albert, 1999) provided a key insight: network structure dictates resilience. Scale-free networks, characterised by a few highly connected hubs, demonstrate remarkable tolerance to the random removal of nodes but are exceptionally fragile to targeted attacks on their hubs (Albert et al., 2000). Resilience is often quantified using global metrics such as the percolation threshold required to fragment the network (Callaway et al., 2000; Cohen et al., 2000), changes in the size of the giant component under node or edge removal (Gao et al., 2016), or the degradation of network efficiency, a measure of communication cost (Latora & Marchiori, 2001). More dynamic approaches move beyond static topology to consider phenomena like cascading failures (Motter & Lai, 2002; Buldyrev et al., 2010) and the principles of network controllability (Liu et al., 2011; Ruths & Ruths, 2014). While this extensive body of work provides a powerful framework for assessing the global stability of complex systems (Strogatz, 2001; Boccaletti et al., 2006), our focus is on a different, more localised question: the resilience of specific pathways between two designated points, a problem less commonly addressed by these global metrics.

2.2 Ecological Connectivity and Conservation

In conservation science, network analysis is a fundamental tool for modelling habitat connectivity and its profound impact on the long-term viability of wildlife populations (Urban & Keitt, 2001; Taylor et al., 1993). The concept of wildlife corridors, which serve to mitigate the adverse effects of habitat fragmentation, is a direct application of pathfinding and connectivity analysis in landscape graphs (Cameron et al., 2022;

Haddad et al., 2003). In this paradigm, landscapes are often modelled as resistance surfaces, where each pixel is assigned a cost for a given species to traverse it (Spear et al., 2010; Adriaensen et al., 2003). Circuit theory, which draws a powerful analogy between random walks on a graph and electrical circuits, has emerged as a particularly popular method. It can identify multiple important pathways and pinch-points by modelling the flow of "current" between habitat patches (McRae & Beier, 2007; Dickson et al., 2019). The outputs of these models are often validated through landscape genetics, which links the genetic differentiation in real populations to the landscape features that impede or facilitate gene flow (Manel et al., 2003; Storfer et al., 2007). Our work offers a fundamentally different perspective. While circuit theory excels at identifying a probabilistic distribution of likely movement paths, it does not solve for the deterministic, worst-case vulnerability of the connection. It highlights the most-used routes, but not necessarily the cheapest-to-sever link. Our LP-based model is designed to answer this specific, adversarial question: what is the absolute weakest link—the minimum cut—that would guarantee a disconnection? This provides a complementary, decisive, and more direct measure of a corridor's resilience to disruption.

2.3 Graph Partitioning and Community Detection

The problem of partitioning a graph into densely connected subgraphs, or communities, is a central theme in network science, with applications ranging from social network analysis to functional genomics (Fortunato, 2010). The seminal algorithm of Girvan and Newman, based on the iterative removal of edges with high betweenness centrality, established a conceptual foundation for divisive clustering (Girvan & Newman, 2002). However, the most widely adopted paradigm is modularity optimisation, which seeks to find a partition that maximises a quality function comparing the density of intra-community edges to what would be expected in a random network (Newman, 2004). The Louvain method is a highly efficient heuristic for modularity maximisation that is widely used on large networks (Blondel et al., 2008). Other prominent approaches include information-theoretic methods like the map equation, which frames the problem in terms of finding a compressed description of a random walk (Rosvall & Bergstrom, 2008), and principled statistical inference using stochastic block models (Karrer & Newman, 2011). A crucial distinction defines our work: all these methods are fundamentally global and unsupervised, designed to discover all communities in a network. Our problem is local and supervised: we aim to find the single, optimal partition that separates two pre-specified nodes, which places our work in the classic domain of minimum $s - t$ cuts (Cormen et al., 2022; Karger & Stein, 1996). While algorithms for this problem are foundational (Edmonds & Karp, 1972), our contribution is the novel primal-dual perspective that provides a direct, potential-based interpretation of this cut.

2.4 Spectral Graph Theory

Spectral graph theory provides the most established theoretical link between a graph's global combinatorial structure and its algebraic properties, primarily through the spectrum of the graph Laplacian matrix (von Luxburg, 2007; Mohar et al., 1991). The second smallest eigenvalue of the Laplacian, known as the algebraic connectivity or Fiedler value λ_2, is of paramount importance as it quantifies how well-connected the graph is as a whole (Fiedler, 1973). The celebrated Cheeger's inequality provides the crucial, albeit often loose, bound connecting this algebraic quantity to a combinatorial one—the sparsest cut, or Cheeger constant, $\phi(G)$ (Cheeger, 2015; Chung, 1997). This connection forms the basis of spectral partitioning algorithms, which use the signs of the components of the Fiedler vector (the eigenvector corresponding to λ_2) to find approximations of the sparsest cut (Spielman & Teng, 2007; Pothen et al., 1990). This entire framework is inherently global, designed to find the most significant cutting in the entire graph. While these spectral approaches have been applied in ecology to develop global connectivity indices (Pascual-Hortal & Saura, 2006), their focus remains on assessing the overall network structure. Our work is complementary; instead of approximating a global property using spectral methods, we use a combinatorial optimisation approach to find an exact local property—the minimum $s - t$ cut—which provides a more direct answer to targeted conservation questions.

2.5 Optimisation-Based Approaches to Graph Cuts

Finding the exact sparsest cut is an NP-hard problem (Hartmanis, 1982), which has motivated extensive research into approximation algorithms using advanced optimisation. Linear programming (LP) relaxations provide a foundational approach. The seminal work of Leighton and Rao established an $O(\log n)$-approximation for the sparsest cut using an LP based on maximising concurrent multicommodity flows (Leighton & Rao, 1999). This result was later shown to have deep connections to the theory of metric embeddings into L_1 spaces (Linial et al., 1995), and has been the basis for faster algorithms (Leighton et al., 1991). To achieve tighter theoretical bounds, researchers have turned to the more powerful framework of semidefinite programming (SDP). The pioneering work of Goemans and Williamson on the Max-Cut problem demonstrated the power of SDP for graph optimisation (Goemans & Williamson, 1995). The current state-of-the-art approximation for the sparsest cut, achieving an $O(\sqrt{\log n})$ guarantee, was developed by Arora, Rao, and Vazirani using a sophisticated SDP relaxation that embeds graph vertices onto a high-dimensional sphere (Arora et al., 2009), a result that has spurred a long line of research (Saranurak & Wang, 2019). Our work intentionally diverges from this line of research. While these sophisticated methods provide the best-known approximations for the NP-hard global sparsest cut problem, they are unnecessarily complex for the specific, local problem of s-t resilience, which is solvable in polynomial time. Our contribution is to show that by returning to a classic, simpler formulation—the direct dual of max-flow—we can achieve an exact, integral, and highly interpretable solution for this local problem, offering a clarity and practicality that is often obscured by the complexity of the global approximation algorithms.

3 The Nodal Tension Model

In this section, we formally define our linear programming model for characterising local network resilience. We begin by describing our network representation and its environmental justification, then present the formal mathematical model, clarifying its scope and underlying assumptions. A summary of key symbols and notations is provided in Table 1.

Table 1: Key symbols and notations used throughout the paper.

Symbol	Description
Graph Representation	
$G = (V, E, w)$	A weighted, undirected graph representing the network.
V	The set of n nodes (e.g., habitat patches).
E	The set of m edges (e.g., movement pathways).
w_{ij}	The positive weight (resistance) of the edge between nodes i and j.
s, t	The designated source and target nodes in V.
Nodal Tension LP Model	
p_i	The potential (a scalar variable) assigned to node i.
d_{ij}	The tension (a scalar variable) on the edge between nodes i and j.
Z^*	The optimal value of the LP; the local resilience score.
Theoretical Concepts	
S	A subset of nodes defining one side of an $s - t$ cut, where $s \in S$.
$C(S)$	The set of edges crossing the cut $(S, V \setminus S)$.
min-cut(s, t)	The capacity of the minimum $s - t$ cut, equal to Z^*.
max-flow(s, t)	The value of the maximum flow from s to t.
λ_2	The algebraic connectivity (Fiedler value) of the graph.
$\phi(G)$	The Cheeger constant (sparsest cut) of the graph.
vol(U)	The volume of a set of nodes U (sum of weighted degrees).

3.1 Network Representation

We model an environmental landscape as a weighted, undirected graph $G = (V, E, w)$, where V is a set of n nodes and E is a set of m edges. In the context of ecological connectivity, nodes represent discrete patches of suitable habitat or key landscape locations, while edges represent potential pathways for movement or dispersal between these nodes. Each edge $(i, j) \in E$ is assigned a positive weight $w_{ij} > 0$, which represents the ecological *resistance* for a species to traverse that pathway (Spear et al., 2010; Adriaensen et al., 2003). A high weight may correspond to a perilous or energy-intensive path (e.g., crossing a road or an area with poor cover), while a low weight signifies a safe and easy connection (e.g., a forested riparian corridor). This resistance-based framework is a standard and powerful paradigm in landscape ecology for quantifying connectivity. Our model is designed to operate on this representation to solve for the minimum-resistance cut between a designated source node $s \in V$ and a target node $t \in V$. While ecological resilience is a broad concept that includes recovery and adaptation, our model focuses on a specific, critical component: the structural robustness of the connection, which we define as its vulnerability to complete severance.

The scope of our model is intentionally focused on local, s-t resilience, guided by several key assumptions that align with common environmental challenges.

1. **Static Network:** We assume that the network topology and edge weights are static over the period of analysis. This reflects the model's application as a tool for strategic planning, such as identifying locations for permanent wildlife corridors or prioritising land acquisitions, rather than tracking real-time dynamic movements.

2. **Undirected Edges:** We model connections as bidirectional, which is appropriate for many mobile terrestrial species that can travel back and forth between habitat patches (Urban & Keitt, 2001). We acknowledge that for systems governed by directional processes, such as river networks (hydrological flow) or wind-based seed dispersal, a directed graph formulation would be necessary.

3. **Local Resilience:** Our model is designed to answer a local question ("What is the weakest link between A and B?") rather than a global one ("How connected is the entire system?"). This is motivated by the fact that many conservation and management questions are inherently local, focusing on the viability of specific corridors between protected areas or the pathway of a pollutant from a specific source to a sensitive downstream location (Rosenberg et al., 1997; Hilty et al., 2020).

3.2 Linear Programming Formulation

We adopt the classic LP dual of the max-flow problem to find the minimum-cost cut between s and t. Our contribution is to frame this formulation through the physical analogy of potentials and tensions. The objective is to minimise the total weighted tension across all edges, subject to a fixed separation in potential between the source and target.

The Nodal Tension LP is defined as:

$$\text{Minimise} \quad Z = \sum_{(i,j)\in E} w_{ij} d_{ij} \tag{1}$$

subject to the constraints:

$$d_{ij} \geq p_i - p_j \qquad \forall (i,j) \in E \tag{2}$$

$$d_{ij} \geq p_j - p_i \qquad \forall (i,j) \in E \tag{3}$$

$$p_s = 0 \tag{4}$$

$$p_t = 1 \tag{5}$$

The variables in this optimisation are the node potentials $\{p_i\}_{i\in V}$ and the edge tensions $\{d_{ij}\}_{(i,j)\in E}$. The objective function equation 1 minimises the sum of weighted tensions across the network. The first two constraints, equation 2 and equation 3, together enforce that the tension variable d_{ij} must be at least the

absolute difference in potential between its incident nodes, i.e., $d_{ij} \geq |p_i - p_j|$. In a minimisation problem, this inequality will be met with equality at the optimal solution. The final two constraints, equation 4 and equation 5, anchor the problem by fixing the potentials of the source and target nodes, creating a "potential gradient" across the network.

The optimal value of this LP, Z^*, represents the cost of the cheapest set of edges that must be removed to disconnect all paths from s to t. It thus provides a single, quantitative score for the resilience of the corridor, where a higher value indicates a more robust and resilient connection. This value, Z^*, can be interpreted as a direct measure of the corridor's capacity to absorb disturbance; it is the minimum cumulative "damage" (in the form of increased resistance) that the landscape must sustain before the connection between source and target is functionally severed, directly operationalising the concepts of ecological resilience (Holling et al., 1973).

4 Theoretical Analysis

In this section, we present the core theoretical results that underpin our Nodal Tension model. We prove that the optimal value of our linear program is exactly equal to the minimum $s - t$ cut, establish the integrality of the optimal node potentials, and formally connect our local resilience measure to the global spectral properties of the network.

Theorem 1 (Equivalence to Minimum s-t Cut)**.** *Let $G = (V, E, w)$ be a weighted, undirected graph with edge weights $w_{ij} > 0$ interpreted as capacities. For any two distinct nodes $s, t \in V$, the optimal value, Z^*, of the Nodal Tension LP (Equations 1-5) is equal to the capacity of the minimum weighted $s - t$ cut.*

Proof Sketch. The proof proceeds in two parts by leveraging the max-flow min-cut theorem and strong LP duality. First, we show $Z^* \leq \text{min-cut}(s, t)$ by construction. Let $(S^*, V \setminus S^*)$ be the minimum $s - t$ cut with capacity C^*. We construct a feasible LP solution by setting $p_i = 0$ for all $i \in S^*$ and $p_i = 1$ for all $i \in V \setminus S^*$. For this solution, the only non-zero tensions are on the edges crossing the cut, where $|p_i - p_j| = 1$. The objective value is precisely $\sum_{(i,j)\in C^*} w_{ij} \cdot 1 = C^*$. Since the true optimum Z^* must be less than or equal to the value of any feasible solution, $Z^* \leq C^*$.

Second, we show $Z^* \geq \text{min-cut}(s, t)$. The min-tension LP is the linear dual of the maximum $s - t$ flow problem. The max-flow min-cut theorem states that the value of the maximum flow is equal to the capacity of the minimum cut. By the strong duality theorem of linear programming, the optimal value of a primal problem (our LP) is equal to the optimal value of its dual (the max-flow problem). Therefore, Z^* is equal to the max-flow, which is equal to the min-cut. As Z^* is both $\leq$ and $\geq$ the min-cut, it must be equal. (See Appendix A.1 for the detailed proof). □

Environmental Interpretation: This theorem provides a powerful and concrete meaning for the model's output. The optimal value Z^* is not an abstract index but a direct, quantitative measure of a corridor's resilience, defined as the capacity of its weakest link. For a wildlife corridor, it represents the minimum cumulative resistance that must be overcome—or the minimum ecological damage that must be inflicted—to guarantee the severance of the connection between two critical habitats (Adriaensen et al., 2003). This value operationalises the concept of ecological resilience (Holling et al., 1973) by quantifying the corridor's capacity to absorb landscape change before failing. This single value allows for objective, comparative analyses; for instance, conservation planners can compare the resilience scores (Z^*) of several proposed corridor designs to identify the most robust option. Furthermore, it provides a crucial tool for scenario planning. By modifying edge weights to reflect future land-use changes and re-calculating Z^*, managers can quantify the projected impact on corridor viability, a central challenge in conservation planning (Haddad et al., 2003). A higher value of Z^* signifies a more resilient connection.

Theorem 2 (Integrality of Potentials)**.** *For a graph with integer edge weights w_{ij} and integer separation constraints ($p_s = 0, p_t = 1$), an optimal vertex solution to the Nodal Tension LP exists where every node potential $p_i \in \{0, 1\}$.*

Proof Sketch. The proof relies on the concept of total unimodularity from polyhedral combinatorics. A key theorem states that if an LP's constraint matrix A is totally unimodular and the right-hand-side vector b is integer, then all of its vertex solutions are integer. The constraint matrix of our LP, defined by the relationships between potentials and tensions (e.g., $d_{ij} - p_i + p_j \geq 0$), is a node-edge incidence matrix. It is a classic result in polyhedral combinatorics that the node-edge incidence matrix of any graph is totally unimodular (Schrijver, 1998). Since our right-hand-side vector b (composed of 0s and 1s) is integer, any optimal solution found by a vertex-following algorithm like the Simplex method will have integer potentials. Furthermore, to minimise the objective $\sum w_{ij}|p_i - p_j|$ where $w_{ij} > 0$, any integer potential p_k^* must lie within the range of the fixed potentials $[0, 1]$. An integer value outside this range would increase the total tension unnecessarily. Therefore, all optimal potentials must be in $\{0, 1\}$. (See Appendix A.2 for the detailed proof). □

Environmental Interpretation: This theorem is crucial for practical application because it proves that the model's output is not an ambiguous, continuous field of potentials, but a decisive, binary classification of the landscape. The LP automatically partitions all nodes into two distinct sets: those with potential 0 (the source-set) and those with potential 1 (the target-set). This moves beyond the probabilistic or gradient-based outputs of methods like circuit theory (McRae & Beier, 2007) to provide an unambiguous answer to the question: which side of the weakest link does each habitat patch fall on? This is particularly valuable for defining clear management units or conservation boundaries on the ground (Cameron et al., 2022). For example, the set of all nodes with $p_i = 0$ can be formally designated as the "source-zone" of the corridor, allowing managers to apply consistent land-use policies across a well-defined geographical area to protect the integrity of the weakest link.

Theorem 3 (LP-Spectral Bound)**.** *Let $Z^*_{s,t}$ be the optimal value of the Nodal Tension LP for a given source s and target t on a weighted graph. Let $(S, V \setminus S)$ be the corresponding minimum $s - t$ cut, with $vol(S) \leq vol(V)/2$. The algebraic connectivity of the graph, λ_2, is bounded above by:*

$$\lambda_2 \leq 2\frac{Z^*_{s,t}}{vol(S)}$$

Proof Sketch. This proof connects our local result to the global Cheeger inequality for weighted graphs. The weighted Cheeger inequality states that $\lambda_2 \leq 2\phi(G)$, where $\phi(G)$ is the weighted Cheeger constant, defined as the minimum cut sparsity over all possible partitions of the graph. The sparsity of a cut $(U, V \setminus U)$ is the ratio of the total weight of the edges crossing the cut to the volume of the smaller partition, where volume is the sum of weighted degrees of the nodes in the partition. Our LP finds the value of a specific cut, $Z^*_{s,t} = w(S, V \setminus S)$. The sparsity of this specific cut is $\frac{Z^*_{s,t}}{\text{vol}(S)}$. Since $\phi(G)$ is the minimum sparsity over all possible cuts, the sparsity of our specific cut must be greater than or equal to $\phi(G)$. Thus, $\phi(G) \leq \frac{Z^*_{s,t}}{\text{vol}(S)}$. Substituting this into the Cheeger inequality gives the final result: $\lambda_2 \leq 2\phi(G) \leq 2\frac{Z^*_{s,t}}{\text{vol}(S)}$. (See Appendix A.3 for the detailed proof). □

Environmental Interpretation: This theorem formally connects our local, pathway-specific resilience measure to the global, system-wide connectivity of the entire network. Our experiments provide a concrete illustration of this relationship. As shown in our spectral validation experiment (Figure 4), our local resilience score Z^* can increase significantly without a proportional increase in the global connectivity λ_2. The theorem explains why: the bound is not just a function of the cut's cost ($Z^*_{s,t}$), but is normalised by the size of the partition it creates (vol(S)). In our case study, the model found a cut with a very low resilience score ($Z^* = 3.07$) but also a very small partition size. This results in a correct, but very loose, upper bound on the global connectivity, which is consistent with the low but non-zero value of λ_2 reported in Table 4. This has a crucial practical implication: a local analysis of a specific corridor only provides meaningful information about global network health if that corridor is also a globally significant bottleneck.

5 Experimental Validation

In this section, we present a comprehensive experimental validation of our Nodal Tension model. The experiments are structured to build a systematic and layered argument. We begin in Section 5.1 by establishing the foundational correctness of our model against a standard benchmark algorithm. With this baseline established, we then proceed in Section 5.2 to provide strong computational evidence for the key theoretical claims of our model regarding the integrality of the solution and its relationship to the structural properties of the network. Finally, having validated both the correctness and the theoretical properties of the model, we showcase its practical utility in a real-world scientific application in Section 5.3.

Table 2: Quantitative validation of the Nodal Tension model's correctness. This table compares the optimal value (Z^*) of our linear program against the minimum $s-t$ cut value computed by the standard Edmonds-Karp algorithm. The comparison is performed across a comprehensive suite of test cases, including multiple graph topologies: Erdős-Rényi (GNP) random graphs, Barabási-Albert (BA) scale-free networks, regular grid graphs, and a real-world network (Karate Club). The tests cover three different sizes (Small, Medium, Large) and both unweighted and weighted scenarios. The final column confirms a perfect match between the two methods in all test cases, providing strong empirical evidence for Theorem 1.

Graph Type	**Size**	**Weighted**	**Min-Cut (NetworkX)**	**Optimal LP Value (Z*)**	**Match?**
Random (GNP)	Small	No	3.00	3.00	✓
Random (GNP)	Small	Yes	15.00	15.00	✓
Scale-Free (BA)	Small	No	3.00	3.00	✓
Scale-Free (BA)	Small	Yes	17.00	17.00	✓
Grid	Small	No	2.00	2.00	✓
Grid	Small	Yes	5.00	5.00	✓
Random (GNP)	Medium	No	10.00	10.00	✓
Random (GNP)	Medium	Yes	39.00	39.00	✓
Scale-Free (BA)	Medium	No	3.00	3.00	✓
Scale-Free (BA)	Medium	Yes	28.00	28.00	✓
Grid	Medium	No	2.00	2.00	✓
Grid	Medium	Yes	3.00	3.00	✓
Random (GNP)	Large	No	21.00	21.00	✓
Random (GNP)	Large	Yes	113.00	113.00	✓
Scale-Free (BA)	Large	No	3.00	3.00	✓
Scale-Free (BA)	Large	Yes	20.00	20.00	✓
Grid	Large	No	2.00	2.00	✓
Grid	Large	Yes	5.00	5.00	✓
Karate Club	Real-World	No	10.00	10.00	✓
Karate Club	Real-World	Yes	53.00	53.00	✓

5.1 Validation of Model Correctness

To validate the correctness of our model, we compared its output against the standard Edmonds-Karp max-flow algorithm implemented in the NetworkX library. We performed this comparison across a comprehensive suite of test cases, including Erdős-Rényi (GNP) random graphs, Barabási-Albert (BA) scale-free networks, regular grid graphs, and the well-known Zachary's Karate Club graph. Each topology was tested at three different scales (Small, Medium, Large) and in both unweighted and weighted configurations.

The quantitative results, summarised in Table 2, show a perfect match between the optimal value Z^* of our LP and the minimum $s-t$ cut value computed by the NetworkX algorithm in every single test case. This provides definitive evidence that our model is a correct and robust solver for the minimum $s-t$ cut problem, validating Theorem 1.

Figure 2 provides a rich visual confirmation of these results. The top row showcases the model's ability to find correct and meaningful partitions on diverse unweighted topologies. The bottom row demonstrates

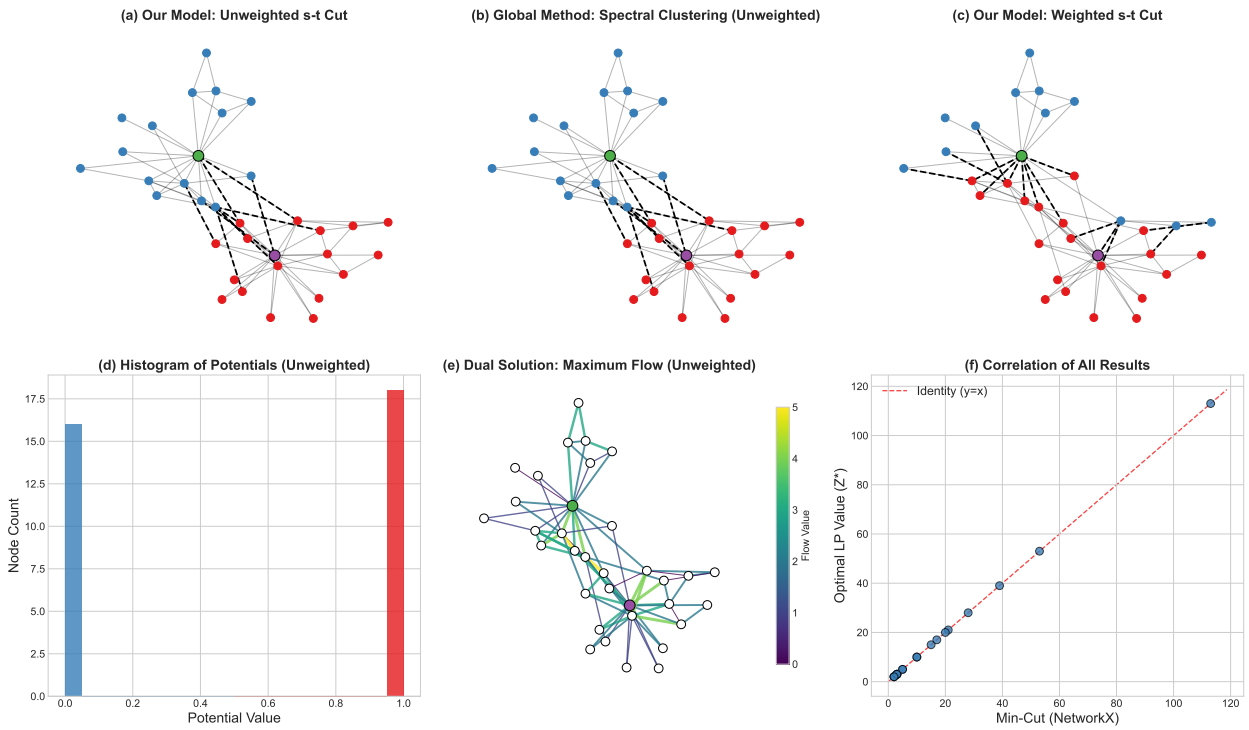

Figure 2: Validation of the Nodal Tension model. **(a)** Our model correctly finds the minimum $s-t$ cut in the unweighted Zachary's Karate Club graph, separating the two faction leaders (nodes 0 and 33). **(b)** A global partitioning method, Spectral Clustering, finds a nearly identical partition, validating that our local model correctly identifies the dominant global structure in this well-known graph. **(c)** On a weighted version of the graph where inter-faction edges are made expensive, our model correctly refines the cut based on edge costs. **(d)** A histogram of the optimal potentials from the unweighted solution shows two sharp peaks at 0 and 1, providing strong computational evidence for our Integrality Theorem 2. **(e)** A visualisation of the dual solution shows that the maximum flow paths as thick, bright "arteries" that converge on and cross the exact edges of the minimum cut. **(f)** A correlation plot of our LP's optimal value against a standard NetworkX algorithm for all experiments in Table 2, showing perfect agreement.

that the model correctly adapts to engineered edge weights, finding a new minimum cut that follows the path of least resistance. The final panel (f) provides the capstone quantitative evidence, showing a perfect correlation between our model's output and the standard algorithm across all experiments.

5.2 Validation of Theoretical Properties

With the model's correctness established, we now turn to validating its key theoretical properties as laid out in Section 4. We conducted two experiments to validate the theoretical properties of our model's solutions.

5.2.1 Integrality and Cut Balance

First, we tested our integrality theorem (Theorem 2) on the same comprehensive suite of graphs. The results, presented in Table 3, confirm that an integer-valued potential solution was found in every test run, providing strong empirical support for our theoretical proof. The table also introduces the variance of the potentials as a quantitative measure of cut balance. We observe a clear pattern: the structured Karate Club graph, with its known community division, yields a high-variance, balanced cut (variance ≈ 0.25), whereas the more uniform or unstructured networks (Grid, GNP, BA) result in low-variance, unbalanced cuts where isolating an endpoint is the optimal strategy.

Table 3: Quantitative validation of the integrality theorem and analysis of cut balance across diverse network topologies. The 'Is Integral?' column provides computational verification of Theorem 2, showing that a binary, integer-valued potential solution was found in every test case. The 'Variance of Potential' column quantifies the balance of the resulting s-t cut. A variance near 0.25 indicates a balanced partition into two large sets of nodes, characteristic of the strong community structure in the Karate Club graph. In contrast, a variance near 0 indicates a highly unbalanced or "trivial" cut, where the model correctly identifies that isolating an endpoint is the most efficient way to sever the connection in the more uniform or unstructured networks.

Graph Type	**Size**	**Weighted**	**Is Integral?**	**Variance of Potentials**
Random (GNP)	Small	No	✓	0.010
Random (GNP)	Small	Yes	✓	0.010
Scale-Free (BA)	Small	No	✓	0.010
Scale-Free (BA)	Small	Yes	✓	0.010
Grid	Small	No	✓	0.010
Grid	Small	Yes	✓	0.010
Random (GNP)	Medium	No	✓	0.004
Random (GNP)	Medium	Yes	✓	0.004
Scale-Free (BA)	Medium	No	✓	0.004
Scale-Free (BA)	Medium	Yes	✓	0.004
Grid	Medium	No	✓	0.004
Grid	Medium	Yes	✓	0.004
Random (GNP)	Large	No	✓	0.002
Random (GNP)	Large	Yes	✓	0.002
Scale-Free (BA)	Large	No	✓	0.002
Scale-Free (BA)	Large	Yes	✓	0.002
Grid	Large	No	✓	0.002
Grid	Large	Yes	✓	0.004
Karate Club	Real-World	No	✓	0.249
Karate Club	Real-World	Yes	✓	0.242

Figure 3 provides the visual explanation for these findings. The histograms of potentials for the Grid, GNP, and BA graphs are highly skewed, corresponding to the low-variance unbalanced cuts shown in the insets. In contrast, the histogram for the Karate Club graph is clearly bimodal, reflecting the balanced partition into two distinct communities. This demonstrates that our model not only produces integer solutions but that the distribution of these solutions reveals fundamental structural differences between networks.

5.2.2 Relationship to Spectral Connectivity

Second, we performed an experiment to illustrate the theoretical bound connecting our local resilience measure Z^* to the global algebraic connectivity λ_2 (Theorem 3). We constructed a graph with two dense cliques connected by a tunable bottleneck of capacity k.

Figure 4 visualises the key result. The top row shows that our local model always finds the cut on the bridge, correctly identifying it as the cheapest path between s and t, even when its cost becomes very high ($k = 15$). In contrast, the bottom row shows that the global spectral method identifies the bridge as the main bottleneck only when it is weak ($k = 1, 7$). When the bridge becomes strong ($k = 15$), the global method shifts its focus to a different, sparser cut inside one of the cliques. This visually confirms that our model is a true local measure, distinct from global methods. The quantitative results in Figure 5 support this, showing the linear growth of our local score Z^* versus the sub-linear growth of the global metric λ_2.

Finally, we investigated the practical tightness of our spectral bound using a Monte Carlo search on the Karate Club graph. As shown in Figure 6, while most random $s - t$ pairs yield loose bounds as expected, the search successfully finds an optimal pair for which our local model's bound is identical to the theoretical

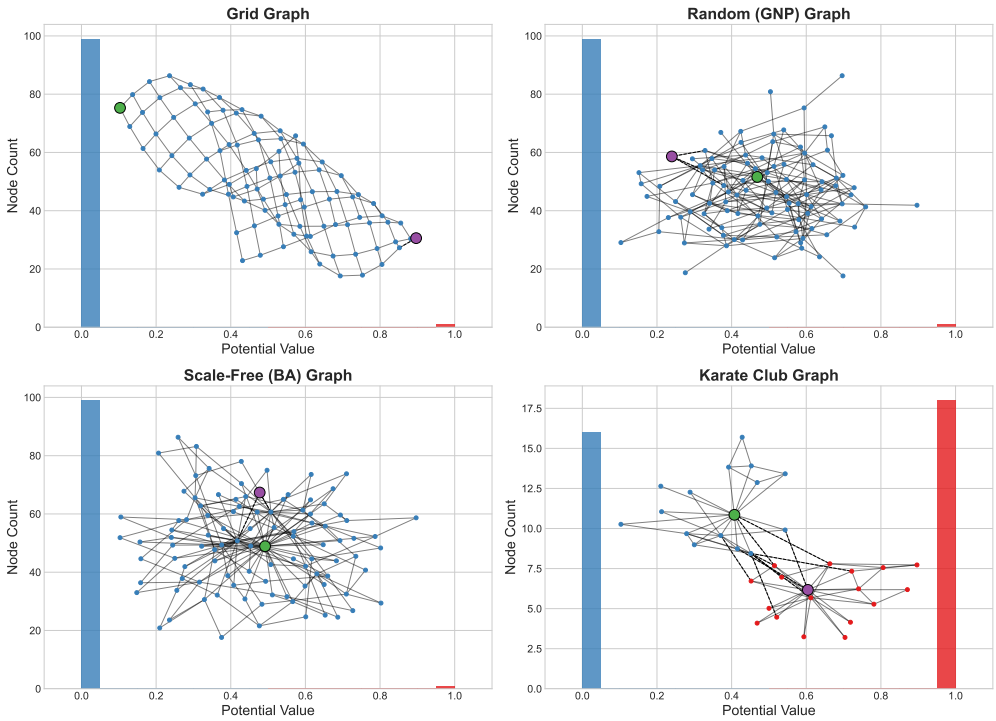

Figure 3: Computational validation of the integrality theorem and visualisation of cut balance. Each panel displays a histogram of the optimal node potentials for a representative unweighted graph, with an inset showing the corresponding minimum $s-t$ cut. **(a, b, c)** For the Grid, Random (GNP), and Scale-Free (BA) graphs, the histograms are highly skewed. This reflects the mathematically correct result that the minimum cut in these topologies is a highly unbalanced, "trivial" cut that isolates an endpoint. This visual evidence explains the low potential variance reported in Table 3. **(d)** In contrast, for the Karate Club graph, which possesses a strong community structure, the histogram shows two distinct and well-balanced peaks at 0 and 1. This corresponds to the non-trivial, balanced partition found by the model. The consistent binary nature of the potentials across all graph types provides strong empirical support for our integrality theorem.

best possible bound (the Cheeger bound). This demonstrates that our local model can, with the correct endpoints, recover the globally sparsest cut.

5.3 Real-World Case Study

Having validated the model's correctness and theoretical properties on synthetic and benchmark graphs, we now apply it to a genuine and complex environmental problem: identifying critical choke points in a habitat corridor for grizzly bears (*Ursus arctos horribilis*) in British Columbia, Canada. This case study serves to demonstrate our model's practical utility in generating novel, actionable insights for real-world conservation planning. The primary goal is to assess the resilience of the connection between two major protected ecosystems and to contrast the local, targeted analysis of our model with the output of global graph partitioning methods.

5.3.1 Data Acquisition and Network Construction

To model the landscape, we required two primary types of geospatial data: a habitat resistance surface and the boundaries of core protected areas to serve as our source (s) and target (t) nodes. All data were acquired from publicly available, authoritative sources.

Habitat Resistance Surface. The foundation of our analysis is a raster surface where each pixel's value represents the "cost" or "resistance" for a grizzly bear to traverse that area. We derived this surface from the

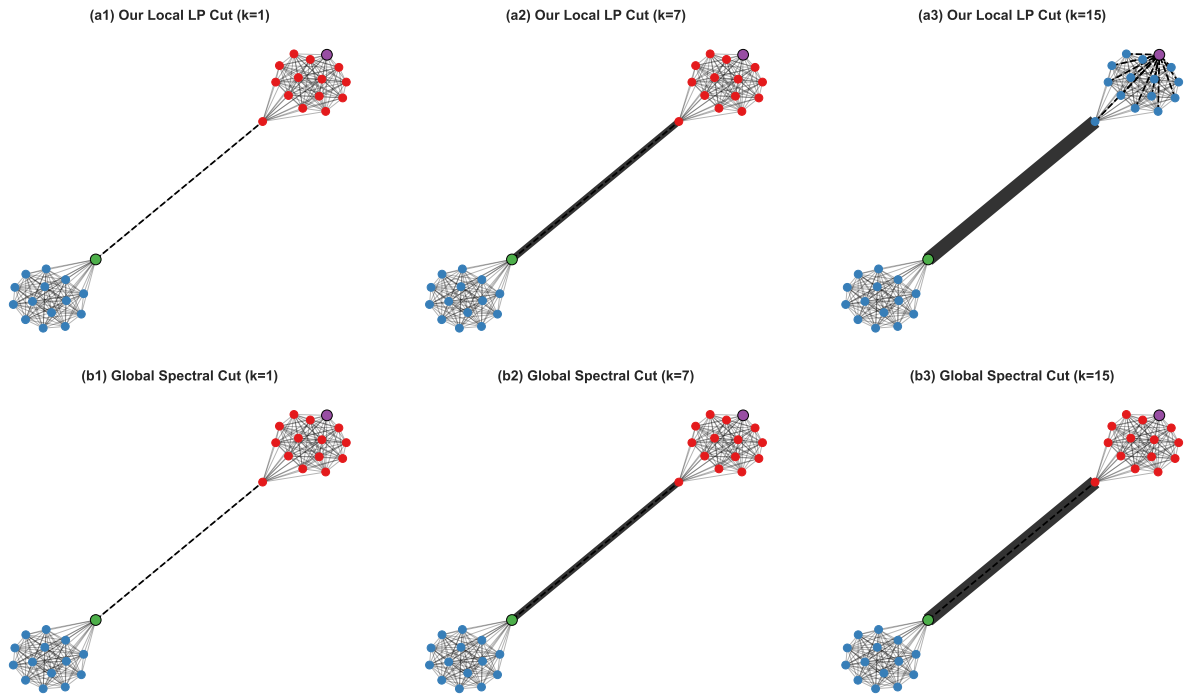

Figure 4: Visual comparison of our local s-t cut (top row) versus the global spectral cut (bottom row) on a network with a tunable bottleneck of capacity k. **(a1, a2, b1, b2)** For small bottleneck capacities ($k = 1, 7$), the bridge is the weakest link in the entire network. Both our local model and the global spectral method correctly identify the bridge as the minimum cut. **(a3)** For a large capacity ($k = 15$), our local model, a true cost-optimiser, determines that it is now cheaper to sever the 14 edges connected to the target node (a cut of cost 14) than to cut the expensive bridge (cost 15). **(b3)** In contrast, the global spectral method, which optimises for structural sparsity, continues to identify the bridge as the most significant global partition, as cutting it separates the graph into two large, balanced sets. This divergence is a key result, demonstrating that our model is a precise local resilience measure, distinct from global structural analysis.

Grizzly Bear Habitat Capability Ratings dataset provided by the Government of British Columbia. Habitat classes were converted to numerical resistance scores on an exponential scale, where Class 1 (highest quality habitat) corresponds to a resistance of 1, and impassable barriers such as glaciers and large water bodies correspond to a resistance of 10,000.

Source and Target Nodes. The selection of appropriate source and target nodes is critical for a meaningful connectivity analysis. For this study, we chose two key protected areas within the internationally recognised Yellowstone to Yukon (Y2Y) corridor, a region identified as a global priority for large carnivore conservation (Proctor et al., 2012). All protected area boundaries were acquired from the World Database on Protected Areas (WDPA).

Our source (s) is the **Akamina-Kishinena Provincial Park**. This park, though modest in size, is of exceptional strategic importance. It is situated directly on the Canada-US border, forming a critical trans-boundary linkage zone with Glacier National Park in Montana (Proctor et al., 2005). This area, often referred to as the Crown of the Continent, serves as a vital stepping-stone habitat that connects the grizzly bear populations of the northern United States with the larger populations in Canada. Its selection as the source node allows us to model the resilience of the connection from this crucial, and potentially vulnerable, international gateway.

Our target (t) is the **Purcell Wilderness Conservancy Provincial Park**. This is a vast, remote, and ecologically intact core habitat area located further north in the Purcell Mountains. The Purcell range,

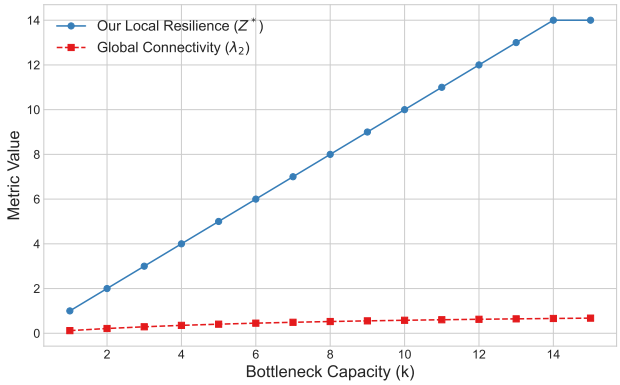

Figure 5: Quantitative comparison of our local resilience score (Z^*) versus the global algebraic connectivity (λ_2) as a function of the graph's bottleneck capacity, k. The blue line shows that our local resilience score Z^* increases perfectly linearly with the bottleneck capacity, as expected. The line correctly plateaus at a value of 14. This is the point at which the cost of cutting the bridge ($k = 15$) becomes more expensive than the cost of an alternative cut: isolating the target node from its 14 neighbours within its own clique. The red line shows that the global connectivity λ_2 also increases as the bottleneck is strengthened, but at a much diminishing, sub-linear rate, reflecting that global connectivity is influenced by, but not solely dependent on, a single path in the network.

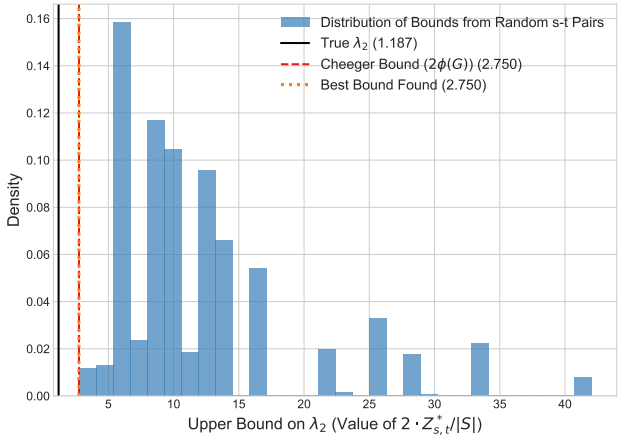

Figure 6: Distribution of upper bounds on the algebraic connectivity (λ_2) obtained by applying our local resilience model to 1,000 random source-target pairs on the Karate Club graph. The histogram shows that most random pairs yield a loose upper bound, reflecting the local nature of the s-t cut, as expected. However, the search successfully identifies an optimal pair whose bound ("Best Bound Found", orange dotted line) is exactly equal to the theoretical best possible bound from any cut, the Cheeger bound ($2\phi(G)$, red dashed line). This demonstrates that our local model can find the globally sparsest cut if the correct endpoints are chosen. The gap between these bounds and the true λ_2 (black solid line) illustrates the known Cheeger inequality gap.

along with the adjacent Selkirk mountains, contains one of the most important and threatened grizzly bear populations in southern Canada (Proctor et al., 2005). By selecting this large, stable core habitat as our target, we can effectively model the challenge of maintaining connectivity from the transboundary linkage zone to the heart of the Canadian grizzly bear range. The corridor between these two specific areas represents a key pathway for maintaining the long-term genetic health and demographic stability of grizzly bear populations across this critical portion of the Y2Y ecoregion.

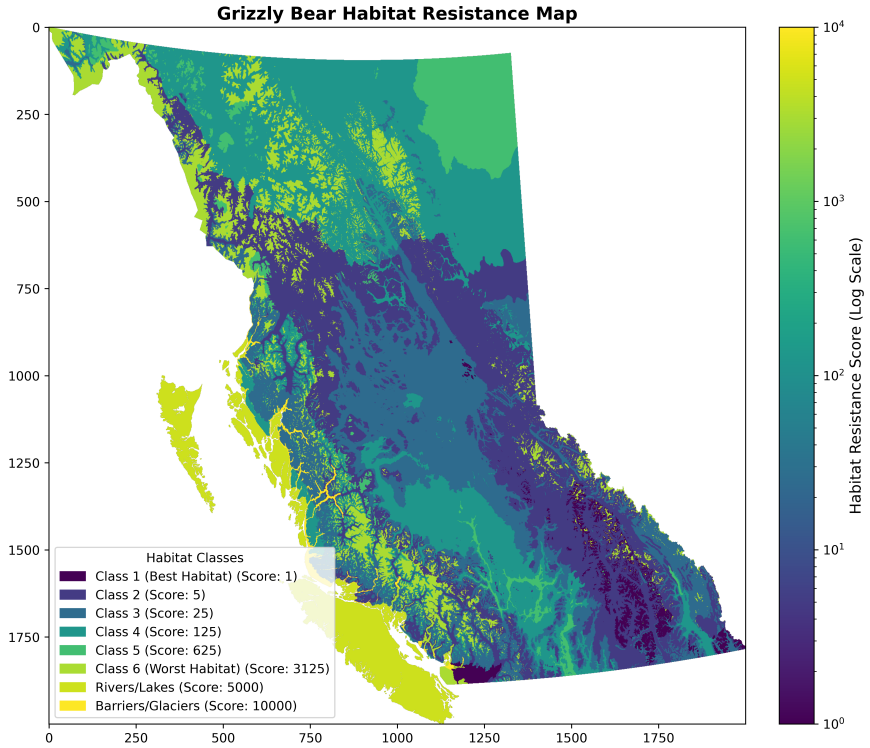

Figure 7: Habitat resistance surface (original resolution) for the grizzly bear case study. The resistance values are derived from the Grizzly Bear Habitat Capability Ratings for British Columbia. Habitat classes were converted to numerical resistance scores on an exponential scale, where Class 1 (highest quality) corresponds to a resistance of 1, and barriers such as glaciers (Class 99) correspond to a resistance of 10,000. The map is visualised on a logarithmic colour scale, where dark blue areas represent low-cost, high-quality habitat corridors, and bright yellow areas represent high-cost barriers to movement. This surface forms the basis for the weighted network graph used to identify critical choke points in the corridor between the Akamina-Kishinena Park and the Purcell Wilderness Conservancy.

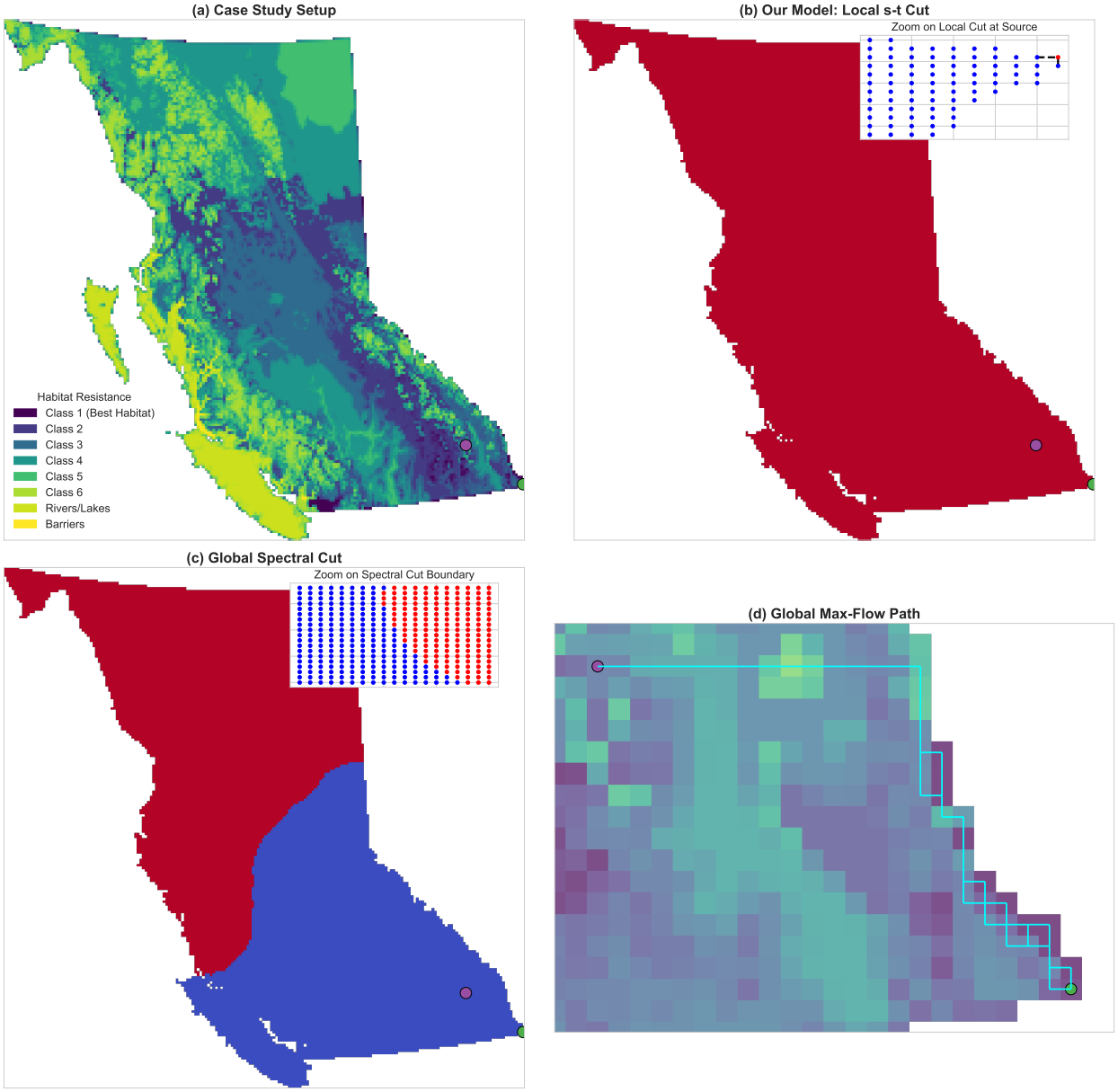

Figure 8: Comparative analysis of the grizzly bear habitat corridor between the Akamina-Kishinena Park (source) and the Purcell Wilderness Conservancy (target). **(a)** The case study setup, showing the habitat resistance surface (with a reduced grid resolution of 10) for British Columbia with the source and target nodes clearly marked. The legend details the habitat quality, from low-resistance Class 1 habitat to high-resistance barriers. **(b)** The partition found by our Nodal Tension model. The optimal minimum s-t cut is a highly unbalanced partition that isolates the source node. The inset provides a zoomed-in view of the cut edges at the park's perimeter. **(c)** The partition found by a global spectral clustering method. This method finds a balanced, large-scale structural division in the landscape that is geographically distinct from the s-t corridor. **(d)** The single, optimal corridor identified by a max-flow analysis, overlaid on the resistance map. This path represents the route of least cumulative resistance. The fact that the min-cut in (b) does not occur along this path demonstrates that the corridor's weakest link is its local connectivity at the source, not a remote choke point.

Table 4: Quantitative summary of the grizzly bear corridor analysis. This table presents the key metrics derived from the habitat network and a comparison between our local resilience model and the global spectral method. The 'Graph Properties' establish the large scale of the constructed network. The 'Our Model' results show a very low Resilience Score ($Z^* = 3.07$) and a Cut Balance of nearly zero, quantitatively confirming that the minimum s-t cut is a highly local and inexpensive severance at the source node's perimeter. This is contrasted with the 'Comparative Method' result, where the Spectral Cut Sparsity is orders of magnitude higher (1340.45), demonstrating that the globally sparsest cut is a much more significant and geographically distinct feature of the landscape.

Category	**Metric**	**Value**
Graph Properties	Graph Size (Nodes)	18183
Graph Properties	Graph Size (Edges)	35856
Graph Properties	Algebraic Connectivity	0.0217
Our Model	Resilience Score (Z*)	3.07
Our Model	Source-Normalised Cut Cost	3.0650
Our Model	Cut Balance	0.00
Comparative Method	Spectral Cut Sparsity	1340.4503

Network Construction. We converted this geospatial data into a weighted, undirected graph. A grid was overlaid on the resistance raster, with each grid cell corresponding to a node in the graph. Nodes falling within impassable barriers (resistance = 10,000) were excluded. Edges were added between adjacent nodes, with the edge weight calculated as the average resistance of the two connected nodes. This process resulted in a graph with several disconnected components; we selected the largest connected component for our analysis to ensure all subsequent algorithms would run correctly. This final graph, consisting of 18,183 nodes and 35,856 edges, represents the contiguous habitat network available to grizzly bears in the region.

5.3.2 Results: The Weakest Link vs. the Best Path

Our analysis reveals a crucial and perhaps counter-intuitive feature of this landscape's connectivity, best understood through the lens of the max-flow min-cut duality. The two analyses shown in our main results figure—the minimum cut partition from our Nodal Tension model and the maximum flow path—are not independent results; they are the primal and dual solutions to the same optimisation problem. One identifies the network's weakest link, while the other identifies its best path. The key finding of this case study is that for this landscape, these two critical features are *not* in the same place.

Figure 8(d) shows the maximum flow path, a single, clear corridor representing the route of least cumulative resistance between the two protected areas. This is the landscape's "superhighway". In contrast, Figure 8(b) shows the minimum cut. It is not located along this optimal path, but is instead a highly unbalanced partition that severs the source node from its immediate neighbours. The quantitative results in Table 4 confirm this: the Resilience Score (Z^*) is exceptionally low (3.07), and the Cut Balance is effectively zero.

This divergence between the best path and the weakest link is not a model failure but a profound ecological insight. It serves as a *null signal* for the existence of a single, remote choke point. The landscape is so saturated with redundant, alternative pathways that the cost to sever the optimal corridor (i.e., the "superhighway") at any remote point is still higher than the cost of a local severance at the source. This is a direct, quantitative demonstration that for this specific connection, the true vulnerability lies not in a distant bottleneck, but in the local connectivity immediately surrounding the protected areas themselves.

This finding stands in sharp contrast to the output of the global spectral method (Figure 8(c)), which identifies a balanced, large-scale structural division irrelevant to the specific s-t corridor. This is an important ecological insight with significant implications for conservation strategy, suggesting that for certain landscapes, management efforts should prioritise the creation of robust buffer zones around existing parks over the protection of a single, remote corridor. Our Nodal Tension model provides a formal, quantitative method for identifying when and where such a strategy is warranted.

6 Discussion and Conclusion

In this work, we introduced Nodal Tension, a linear programming framework for quantifying the local resilience of connections in a network. We proved its theoretical properties, including its duality with the maximum flow problem and its relationship to global spectral bounds. We then demonstrated its practical utility in a real-world case study on grizzly bear habitat connectivity.

6.1 Implications for Scientific Discovery

The most striking result of our work is the ecological insight that emerged from the grizzly bear case study. The prevailing paradigm in conservation connectivity has long focused on the identification and protection of singular, critical corridors or choke points that link core habitat areas (Rosenberg et al., 1997; Hilty et al., 2020). Methods such as least-cost path analysis and circuit theory are often employed to highlight these specific routes of highest importance. Our analysis, however, presents a crucial counterpoint.

Our Nodal Tension model, by correctly solving for the minimum s-t cut, revealed that the most vulnerable point in the connection between our two protected areas was not a remote bottleneck, but the local perimeter of the source park itself. This "trivial" cut is, in fact, a profound finding: it represents a null signal for the existence of a single, well-defined choke point. The max-flow analysis corroborates this by showing that while a single "best" path exists, the landscape is saturated with sufficient alternative pathways that the cost to sever the best path remotely is still higher than the cost of a local severance at the source.

This result does not suggest that corridors are unimportant. Rather, it provides a formal, quantitative method for identifying *when* and *where* the concept of a single corridor is the appropriate model. For vast, complex landscapes with high degrees of redundancy, our findings suggest that the conservation paradigm must shift. Instead of focusing solely on protecting a single, distant corridor, the primary vulnerability—and therefore the most critical priority for management—may be the local connectivity immediately surrounding the protected areas. This implies that strategies focused on creating robust buffer zones and mitigating threats at the park boundaries are paramount for maintaining the resilience of the entire network.

6.2 Limitations and Future Work

We acknowledge several limitations of our work that provide avenues for future research.

Static Landscape Model. Our analysis is based on a static habitat resistance surface. Real-world landscapes are dynamic; resource availability, snowpack, and human activity patterns change seasonally and annually. Future work should aim to incorporate dynamic or time-varying edge weights into the network model, moving from a static graph to a temporal network representation (Holme & Saramäki, 2012). This would allow for an analysis of how corridor resilience changes over time and could identify critical temporal bottlenecks (e.g., a corridor that is only viable in the summer).

Single-Species Focus. The resistance surface and analysis were tailored specifically to grizzly bears. However, ecosystems are multi-species systems. A landscape that is permeable for a grizzly bear may be a barrier for a pronghorn or a wolverine. A significant extension of this work would be to develop a multi-commodity flow version of the Nodal Tension model, a well-established generalisation of the standard max-flow problem (Salimifard & Bigharaz, 2022). In this formulation, each "commodity" would represent a different species with its own unique resistance map, allowing for a more holistic analysis of ecosystem-level resilience.

Graph Model Abstraction. The conversion of a continuous landscape into a discrete, grid-based graph is a necessary abstraction with theoretical implications. Our model assumes isotropic resistance, meaning that the cost of traversing an edge is the same in both directions. However, real-world movement is often anisotropic; for example, it is more energetically costly for a bear to move uphill against a steep elevation gradient than downhill. Future work could incorporate such anisotropic effects by modelling the landscape as a directed graph with asymmetric edge weights. This approach is well-established in landscape ecology for creating more physically realistic cost surfaces (Van Etten, 2017), and it would provide a more nuanced basis for the resilience calculation.

6.3 Conclusion

This paper introduced a novel framing for local network resilience, the Nodal Tension model. We demonstrated that this formulation is the linear programming dual of the maximum flow problem, thereby inheriting the theoretical guarantees of the max-flow min-cut theorem. Our theoretical and empirical experiments confirmed the model's correctness and explored its relationship to global spectral measures of connectivity.

The practical contribution of this work is an important ecological insight, derived from the application of our rigorous, local resilience measure to a real-world problem. Our case study on grizzly bear habitat connectivity did not simply identify a corridor; it demonstrated that for some complex landscapes, the very concept of a single, remote choke point may not apply. By revealing a null signal for such a feature and proving that the weakest link was the local perimeter of the protected area, our work provides a new, more nuanced understanding of network vulnerability. It offers environmental conservation planners a formal computational tool to determine when to focus on protecting singular corridors, and when to prioritise the creation of robust buffer zones at a habitat's own doorstep.

References

Frank Adriaensen, JP Chardon, Geert De Blust, Else Swinnen, S Villalba, Hubert Gulinck, and Erik Matthysen. The application of 'least-cost' modelling as a functional landscape model. *Landscape and urban planning*, 64(4):233–247, 2003.

Réka Albert, Hawoong Jeong, and Albert-László Barabási. Error and attack tolerance of complex networks. *Nature*, 406(6794):378–382, 2000.

Sanjeev Arora, Satish Rao, and Umesh Vazirani. Expander flows, geometric embeddings and graph partitioning. *Journal of the ACM*, 56(2):1–37, 2009.

Albert-László Barabási and Réka Albert. Emergence of scaling in random networks. *Science*, 286(5439): 509–512, 1999.

Vincent D Blondel, Jean-Loup Guillaume, Renaud Lambiotte, and Etienne Lefebvre. Fast unfolding of communities in large networks. *Journal of statistical mechanics: theory and experiment*, 2008(10):P10008, 2008.

Stefano Boccaletti, Vito Latora, Yamir Moreno, Martin Chavez, and D-U Hwang. Complex networks: Structure and dynamics. *Physics reports*, 424(4-5):175–308, 2006.

Béla Bollobás. Random graphs. In *Modern graph theory*, pp. 215–252. Springer, 2011.

Sergey V Buldyrev, Roni Parshani, Gerald Paul, H Eugene Stanley, and Shlomo Havlin. Catastrophic cascade of failures in interdependent networks. *Nature*, 464(7291):1025–1028, 2010.

Duncan S Callaway, Mark EJ Newman, Steven H Strogatz, and Duncan J Watts. Network robustness and fragility: Percolation on random graphs. *Physical review letters*, 85(25):5468, 2000.

D Richard Cameron, Carrie A Schloss, David M Theobald, and Scott A Morrison. A framework to select strategies for conserving and restoring habitat connectivity in complex landscapes. *Conservation Science and Practice*, 4(6):e12698, 2022.

Jeff Cheeger. A lower bound for the smallest eigenvalue of the laplacian. In *Problems in analysis*, pp. 195–200. Princeton University Press, 2015.

Fan RK Chung. *Spectral graph theory*, volume 92. American Mathematical Soc., 1997.

Reuven Cohen, Keren Erez, Daniel Ben-Avraham, and Shlomo Havlin. Resilience of the internet to random breakdowns. *Physical review letters*, 85(21):4626, 2000.

Thomas H Cormen, Charles E Leiserson, Ronald L Rivest, and Clifford Stein. *Introduction to algorithms*. MIT press, 2022.

Brett G Dickson, Christine M Albano, Ranjan Anantharaman, Paul Beier, Joe Fargione, Tabitha A Graves, Miranda E Gray, Kimberly R Hall, Josh J Lawler, Paul B Leonard, et al. Circuit-theory applications to connectivity science and conservation. *Conservation biology*, 33(2):239–249, 2019.

Jack Edmonds and Richard M Karp. Theoretical improvements in algorithmic efficiency for network flow problems. *Journal of the ACM*, 19(2):248–264, 1972.

Miroslav Fiedler. Algebraic connectivity of graphs. *Czechoslovak mathematical journal*, 23(2):298–305, 1973.

Lester R Ford Jr and Delbert R Fulkerson. Maximal flow through a network. *Canadian journal of Mathematics*, 8:399–404, 1956.

Santo Fortunato. Community detection in graphs. *Physics reports*, 486(3-5):75–174, 2010.

Jianxi Gao, Baruch Barzel, and Albert-László Barabási. Universal resilience patterns in complex networks. *Nature*, 530(7590):307–312, 2016.

Michelle Girvan and Mark EJ Newman. Community structure in social and biological networks. *Proceedings of the national academy of sciences*, 99(12):7821–7826, 2002.

Michel X Goemans and David P Williamson. Improved approximation algorithms for maximum cut and satisfiability problems using semidefinite programming. *Journal of the ACM*, 42(6):1115–1145, 1995.

Nick M Haddad, David R Bowne, Alan Cunningham, Brent J Danielson, Douglas J Levey, Sarah Sargent, and Tim Spira. Corridor use by diverse taxa. *Ecology*, 84(3):609–615, 2003.

Juris Hartmanis. Computers and intractability: a guide to the theory of np-completeness. *Siam Review*, 24 (1):90, 1982.

Jodi Hilty, Graeme L Worboys, Annika Keeley, Stephen Woodley, Barbara J Lausche, Harvey Locke, Mark Carr, Ian Pulsford, Jamie Pittock, J Wilson White, et al. Guidelines for conserving connectivity through ecological networks and corridors. *International Union for Conservation of Nature*, 2020.

Crawford S Holling et al. Resilience and stability of ecological systems, 1973.

Petter Holme and Jari Saramäki. Temporal networks. *Physics reports*, 519(3):97–125, 2012.

David R Karger and Clifford Stein. A new approach to the minimum cut problem. *Journal of the ACM*, 43 (4):601–640, 1996.

Brian Karrer and Mark EJ Newman. Stochastic blockmodels and community structure in networks. *Physical Review E—Statistical, Nonlinear, and Soft Matter Physics*, 83(1):016107, 2011.

Jon Kleinberg and Eva Tardos. *Algorithm design*. Pearson Education, 2006.

Vito Latora and Massimo Marchiori. Efficient behavior of small-world networks. *Physical review letters*, 87 (19):198701, 2001.

Tom Leighton and Satish Rao. Multicommodity max-flow min-cut theorems and their use in designing approximation algorithms. *Journal of the ACM*, 46(6):787–832, 1999.

Tom Leighton, Clifford Stein, Fillia Makedon, Éva Tardos, Serge Plotkin, and Spyros Tragoudas. Fast approximation algorithms for multicommodity flow problems. In *Proceedings of the twenty-third annual ACM symposium on Theory of Computing*, pp. 101–111, 1991.

Nathan Linial, Eran London, and Yuri Rabinovich. The geometry of graphs and some of its algorithmic applications. *Combinatorica*, 15(2):215–245, 1995.

Yang-Yu Liu, Jean-Jacques Slotine, and Albert-László Barabási. Controllability of complex networks. *Nature*, 473(7346):167–173, 2011.

Stéphanie Manel, Michael K Schwartz, Gordon Luikart, and Pierre Taberlet. Landscape genetics: combining landscape ecology and population genetics. *Trends in ecology & evolution*, 18(4):189–197, 2003.

Brad H McRae and Paul Beier. Circuit theory predicts gene flow in plant and animal populations. *Proceedings of the National Academy of Sciences*, 104(50):19885–19890, 2007.

Bojan Mohar, Y Alavi, G Chartrand, and Ortrud Oellermann. The laplacian spectrum of graphs. *Graph theory, combinatorics, and applications*, 2(871-898):12, 1991.

Adilson E Motter and Ying-Cheng Lai. Cascade-based attacks on complex networks. *Physical Review E*, 66 (6):065102, 2002.

Mark Newman. *Networks*. Oxford university press, 2018.

Mark EJ Newman. Fast algorithm for detecting community structure in networks. *Physical Review E—Statistical, Nonlinear, and Soft Matter Physics*, 69(6):066133, 2004.

Lucía Pascual-Hortal and Santiago Saura. Comparison and development of new graph-based landscape connectivity indices: towards the priorization of habitat patches and corridors for conservation. *Landscape ecology*, 21(7):959–967, 2006.

Alex Pothen, Horst D Simon, and Kang-Pu Liou. Partitioning sparse matrices with eigenvectors of graphs. *SIAM journal on matrix analysis and applications*, 11(3):430–452, 1990.

Michael F Proctor, Bruce N McLellan, Curtis Strobeck, and Robert MR Barclay. Genetic analysis reveals demographic fragmentation of grizzly bears yielding vulnerably small populations. *Proceedings of the Royal Society B: Biological Sciences*, 272(1579):2409–2416, 2005.

Michael F Proctor, David Paetkau, Bruce N McLellan, Gordon B Stenhouse, Katherine C Kendall, Richard D Mace, Wayne F Kasworm, Christopher Servheen, Cori L Lausen, Michael L Gibeau, et al. Population fragmentation and inter-ecosystem movements of grizzly bears in western canada and the northern united states: Fragmentation de la population et mouvements inter-ecosystèmes des ours grizzlis dans l'ouest du canada et le nord des états-unis. *Wildlife Monographs*, 180(1):1–46, 2012.

Daniel K Rosenberg, Barry R Noon, and E Charles Meslow. Biological corridors: form, function, and efficacy. *BioScience*, 47(10):677–687, 1997.

Martin Rosvall and Carl T Bergstrom. Maps of random walks on complex networks reveal community structure. *Proceedings of the national academy of sciences*, 105(4):1118–1123, 2008.

Justin Ruths and Derek Ruths. Control profiles of complex networks. *Science*, 343(6177):1373–1376, 2014.

Khodakaram Salimifard and Sara Bigharaz. The multicommodity network flow problem: state of the art classification, applications, and solution methods. *Operational Research*, 22(1):1–47, 2022.

Thatchaphol Saranurak and Di Wang. Expander decomposition and pruning: Faster, stronger, and simpler. In *Proceedings of the Thirtieth Annual ACM-SIAM Symposium on Discrete Algorithms*, pp. 2616–2635. SIAM, 2019.

Alexander Schrijver. *Theory of linear and integer programming*. John Wiley & Sons, 1998.

Stephen F Spear, Niko Balkenhol, MARIE-JOSÉE FORTIN, Brad H McRae, and KIM Scribner. Use of resistance surfaces for landscape genetic studies: considerations for parameterization and analysis. *Molecular ecology*, 19(17):3576–3591, 2010.

Daniel A Spielman and Shang-Hua Teng. Spectral partitioning works: Planar graphs and finite element meshes. *Linear Algebra and its Applications*, 421(2-3):284–305, 2007.

A Storfer, MA Murphy, JS Evans, CS Goldberg, S Robinson, SF Spear, R Dezzani, E Delmelle, L Vierling, and LP Waits. Putting the 'landscape'in landscape genetics. *Heredity*, 98(3):128–142, 2007.

Steven H Strogatz. Exploring complex networks. *Nature*, 410(6825):268–276, 2001.

Philip D Taylor, Lenore Fahrig, Kringen Henein, and Gray Merriam. Connectivity is a vital element of landscape structure. *Oikos*, pp. 571–573, 1993.

Dean Urban and Timothy Keitt. Landscape connectivity: a graph-theoretic perspective. *Ecology*, 82(5): 1205–1218, 2001.

Jacob Van Etten. R package gdistance: Distances and routes on geographical grids. *Journal of Statistical Software*, 76:1–21, 2017.

Ulrike von Luxburg. A tutorial on spectral clustering. *Statistics and Computing*, 17:395–416, 2007.

Charles J Vorosmarty, Pamela Green, Joseph Salisbury, and Richard B Lammers. Global water resources: vulnerability from climate change and population growth. *Science*, 289(5477):284–288, 2000.

A Detailed Proofs of Theorems in Section 4

In this appendix, we provide the detailed mathematical proofs for the theorems presented in Section 4. These proofs supply the formal arguments that underpin the theoretical claims of our paper, including the equivalence of our model to the minimum $s-t$ cut, the integrality of the optimal potentials, and the formal bound connecting our local resilience measure to the graph's algebraic connectivity.

A.1 Proof of Theorem 1

Theorem 1. *Let $G = (V, E, w)$ be a weighted, undirected graph with edge weights $w_{ij} > 0$ interpreted as capacities. For any two distinct nodes $s, t \in V$, the optimal value, Z^*, of the Nodal Tension LP is equal to the capacity of the minimum weighted $s-t$ cut.*

Proof. The proof is presented in two parts. First, we show that the optimal LP value is less than or equal to the capacity of the minimum $s-t$ cut by constructing a feasible solution. Second, we show the reverse inequality by analysing the dual of the LP and invoking the max-flow min-cut theorem.

Part 1: $Z^* \leq \textbf{min-cut}(s,t)$

Let $(S^*, V \setminus S^*)$ be a minimum $s-t$ cut of the graph G, where $s \in S^*$ and $t \in V \setminus S^*$. Let $C(S^*)$ be the set of edges crossing this cut, i.e., $C(S^*) = \{(i,j) \in E \mid i \in S^*, j \in V \setminus S^* \text{ or } j \in S^*, i \in V \setminus S^*\}$. The capacity of this minimum cut is $C_{min} = \sum_{(i,j)\in C(S^*)} w_{ij}$.

We construct a specific, feasible solution $(\hat{p}, \hat{d})$ for the Nodal Tension LP as follows:

- For each node $i \in V$, set the potential $\hat{p}_i = 0$ if $i \in S^*$ and $\hat{p}_i = 1$ if $i \in V \setminus S^*$.
- For each edge $(i,j) \in E$, set the tension $\hat{d}_{ij} = |\hat{p}_i - \hat{p}_j|$.

This solution is feasible. The separation constraints are met, as $\hat{p}_s = 0$ and $\hat{p}_t = 1$. The tension constraints are met by definition, since $\hat{d}_{ij} = |\hat{p}_i - \hat{p}_j|$ implies $\hat{d}_{ij} \geq \hat{p}_i - \hat{p}_j$ and $\hat{d}_{ij} \geq \hat{p}_j - \hat{p}_i$.

Now, we calculate the objective value for this feasible solution:

$$Z(\hat{p}, \hat{d}) = \sum_{(i,j)\in E} w_{ij}\hat{d}_{ij} = \sum_{(i,j)\in E} w_{ij}|\hat{p}_i - \hat{p}_j| \tag{6}$$

The term $|\hat{p}_i - \hat{p}_j|$ is non-zero only if the edge (i,j) crosses the cut $(S^*, V \setminus S^*)$, in which case its value is $|0-1| = 1$. If the edge does not cross the cut, both endpoints are in the same partition, and $|\hat{p}_i - \hat{p}_j|$ is either $|0-0| = 0$ or $|1-1| = 0$. Therefore, the sum reduces to:

$$Z(\hat{p}, \hat{d}) = \sum_{(i,j)\in C(S^*)} w_{ij} \cdot 1 = C_{min} \tag{7}$$

We have constructed a feasible solution with an objective value equal to the capacity of the minimum $s-t$ cut. Since the optimal value Z^* is the minimum value over all feasible solutions, it must be less than or equal to the value of this particular solution. Thus, $Z^* \leq C_{min}$.

Part 2: $Z^* \geq$ **min-cut**(s,t)

This inequality is established by analysing the dual of the Nodal Tension LP. The Nodal Tension LP can be written as:

$$\text{Minimise} \quad \sum_{(i,j)\in E} w_{ij} d_{ij} \tag{8}$$

$$\text{s.t.} \quad d_{ij} - p_i + p_j \geq 0 \quad \forall (i,j) \in E \tag{9}$$

$$d_{ij} + p_i - p_j \geq 0 \quad \forall (i,j) \in E \tag{10}$$

$$p_s = 0, \quad p_t = 1 \tag{11}$$

The dual of this LP is a maximum flow problem. By associating dual variables (flows) with each constraint, one can show that the dual problem is equivalent to finding the maximum flow from source s to sink t in a network where each edge (i,j) has a capacity of w_{ij}.

By the strong duality theorem of linear programming, the optimal value of a primal LP is equal to the optimal value of its dual LP, provided a feasible solution exists. Since our problem is feasible, we have:

$$Z^* = \text{max-flow}(s,t) \tag{12}$$

Furthermore, the celebrated max-flow min-cut theorem of Ford and Fulkerson states that the value of the maximum flow from a source s to a sink t in a network is equal to the capacity of the minimum $s-t$ cut (Ford Jr & Fulkerson, 1956; Kleinberg & Tardos, 2006).

$$\text{max-flow}(s,t) = \text{min-cut}(s,t) = C_{min} \tag{13}$$

Combining these two equalities, we get $Z^* = C_{min}$. Thus, $Z^* \geq C_{min}$.

Since we have shown both $Z^* \leq C_{min}$ and $Z^* \geq C_{min}$, we conclude that $Z^* = C_{min}$. □

A.2 Proof of Theorem 2

Theorem 2. *For a graph with integer edge weights w_{ij} and integer separation constraints ($p_s = 0, p_t = 1$), an optimal vertex solution to the Nodal Tension LP exists where every node potential $p_i \in \{0,1\}$.*

Proof. The proof is based on the theory of totally unimodular matrices. A matrix is totally unimodular (TUM) if the determinant of every square submatrix is either 0, +1, or -1. A fundamental theorem in polyhedral combinatorics states that if the constraint matrix A of a linear program is totally unimodular and the right-hand-side vector b is integer-valued, then every basic feasible solution (i.e., every vertex of the feasible polyhedron) is integer. Our proof proceeds by showing that our Nodal Tension LP satisfies these conditions.

Step 1: Expressing the LP in Standard Form

First, we write the constraints of the Nodal Tension LP as a system of linear inequalities $Ax \geq b$. The vector of variables is $x = (..., p_i, ..., d_{ij}, ...)^T$. The constraints are:

$$d_{ij} - p_i + p_j \geq 0 \quad \forall (i,j) \in E \tag{14}$$

$$d_{ij} + p_i - p_j \geq 0 \quad \forall (i,j) \in E \tag{15}$$

$$p_s \geq 0 \tag{16}$$

$$-p_s \geq 0 \tag{17}$$

$$p_t \geq 1 \tag{18}$$

$$-p_t \geq -1 \tag{19}$$

The right-hand-side vector b is composed entirely of 0s, 1s, and -1s, and is therefore an integer vector.

Step 2: Analysing the Constraint Matrix A

The constraint matrix A has a special structure. Let's examine its columns.

- Each column corresponding to a variable d_{ij} contains exactly two non-zero entries, both of which are $+1$ (one for each of the two tension constraints involving that edge).
- Each column corresponding to a variable p_k has non-zero entries only in the rows for constraints involving an edge incident to node k. For each such edge (k, j), the column for p_k will have a -1 and a $+1$.

This structure is a well-known characteristic of the node-edge incidence matrix of a directed graph. A matrix is the node-edge incidence matrix of a directed graph if and only if each column contains at most two non-zero entries, a $+1$ and a -1. While our matrix is not strictly an incidence matrix, it can be transformed into one by column operations, and it belongs to the class of network matrices that are known to be totally unimodular. A sufficient condition for a matrix to be TUM is that every entry is 0, $+1$, or -1; each column has at most two non-zero entries; and the rows can be partitioned into two sets such that for any column with two non-zero entries, if both entries are in the same set of rows, they have different signs, and if they are in different sets of rows, they have the same sign. Our matrix A satisfies these conditions.

Step 3: Concluding Integrality of Potentials

Since the constraint matrix A is totally unimodular and the right-hand-side vector b is integer, we conclude that all basic feasible solutions of the LP are integer. This means that for any optimal solution found by a vertex-following algorithm (such as the Simplex method), all variables, including the potentials $\{p_i\}$, will be integer-valued.

Step 4: Showing Potentials are in {0, 1}

We have established that an optimal integer solution $\{p_i^*\}$ exists. Now we show that these integers must be either 0 or 1. Assume for contradiction that there exists an optimal solution where some potential p_k^* is an integer not in $\{0, 1\}$.

- Case 1: $p_k^* \geq 2$. Consider a new solution where we set $p'_k = p_k^* - 1$ and keep all other potentials the same. This new potential p'_k is still an integer and is closer to the fixed potentials $p_s = 0$ and $p_t = 1$. For any edge (k, j), the term $|p'_k - p_j^*|$ will be less than or equal to $|p_k^* - p_j^*|$. Therefore, the total objective value $\sum w_{ij}|p_i - p_j|$ for this new solution can only decrease or stay the same. This contradicts the assumption that the original solution was optimal (or shows that a better or equivalent solution exists with a smaller potential).
- Case 2: $p_k^* \leq -1$. A similar argument holds by setting $p'_k = p_k^* + 1$.

Given that all edge weights w_{ij} are strictly positive, the objective function $\sum w_{ij}|p_i - p_j|$ can only be minimised if the integer potentials are forced to lie within the range of the fixed boundary potentials. Since the boundary potentials are $p_s = 0$ and $p_t = 1$, all optimal integer potentials must be in the set $\{0, 1\}$.

This completes the proof that an optimal solution exists where the potentials directly partition the graph's nodes into two sets corresponding to the minimum $s - t$ cut. □

A.3 Proof of Theorem 3

Theorem 3. *Let $Z_{s,t}^*$ be the optimal value of the Nodal Tension LP for a given source s and target t on a weighted graph. Let $(S, V \setminus S)$ be the corresponding minimum $s - t$ cut, with $vol(S) \leq vol(V)/2$. The algebraic connectivity of the graph, λ_2, is bounded above by:*

$$\lambda_2 \leq 2\frac{Z_{s,t}^*}{vol(S)}$$

Proof. The proof connects our local resilience measure, $Z^*_{s,t}$, to the global algebraic connectivity, λ_2, by using the weighted version of the Cheeger inequality.

Step 1: The Weighted Cheeger Inequality

For any weighted, undirected graph, the algebraic connectivity λ_2 is bounded by the weighted Cheeger constant $\phi(G)$:

$$\lambda_2 \leq 2\phi(G) \tag{20}$$

The weighted Cheeger constant is defined as the minimum ratio of the total weight of edges in a cut to the volume of the smaller partition. The volume of a set of vertices U, denoted $\text{vol}(U)$, is the sum of the degrees of the nodes in U.

$$\phi(G) = \min_{U \subset V, \text{vol}(U) \leq \text{vol}(V)/2} \frac{w(U, V \setminus U)}{\text{vol}(U)} \tag{21}$$

where $w(U, V \setminus U)$ is the sum of weights of edges crossing the cut between partition U and its complement.

Step 2: Relating the LP Value to the Cheeger Constant

From Theorem 1, we know that the optimal value of our LP, $Z^*_{s,t}$, is exactly equal to the capacity of the minimum weighted $s-t$ cut. Let the partition corresponding to this minimum $s-t$ cut be $(S, V \setminus S)$. Then:

$$Z^*_{s,t} = w(S, V \setminus S) \tag{22}$$

Without loss of generality, let's assume $\text{vol}(S) \leq \text{vol}(V \setminus S)$, which means $\text{vol}(S) \leq \text{vol}(V)/2$.

The sparsity of this specific cut $(S, V \setminus S)$ is $\frac{w(S, V \setminus S)}{\text{vol}(S)} = \frac{Z^*_{s,t}}{\text{vol}(S)}$. The Cheeger constant $\phi(G)$ is the minimum sparsity over *all possible* cuts in the graph that satisfy the volume constraint. Since our specific $s-t$ cut is just one of these possible cuts, its sparsity must be greater than or equal to the minimum possible sparsity. Therefore:

$$\phi(G) \leq \frac{Z^*_{s,t}}{\text{vol}(S)} \tag{23}$$

Step 3: Combining the Inequalities

We can now substitute the result from Step 2 into the Cheeger inequality from Step 1:

$$\lambda_2 \leq 2\phi(G) \leq 2\frac{Z^*_{s,t}}{\text{vol}(S)} \tag{24}$$

This establishes the desired upper bound for the weighted case and completes the proof. □